JOURNAL OF CATALYSIS 144, 352–357 (1993)

The Role of Lattice Oxygen during the Oxidative Coupling of Methane over Li^+-Doped TiO_2 Catalysts

The influence of surface promoters and dopants on the catalytic performance of TiO_2 and other rare-earth oxides in the oxidative coupling of methane (OCM) has gained significant interest among many investigators (*1, 2*). Altervalent cation doping of metal oxides involves incorporation of foreign cations of valence lower or higher than that of the parent cation into the crystal structure of the parent oxide. As a result of this process, the electron structure (Fermi energy level) (*3*), acidity/basicity characteristics (*2, 4*), and oxygen anion mobility (*5, 6*) are altered. These parameters are expected to influence catalytic rates of surface reactions, which in turn, control activity and selectivity parameters. It is very desirable then to investigate the intrinsic correlations of the aforementioned parameters with those of catalyst performance, if any exist. Further, this information has to be obtained under experimental conditions similar to those employed for measurements of kinetic parameters. In the case of the OCM reaction this may not be an easy task.

The present work aims towards the establishment of a fundamental understanding of what might be the role of lattice oxygen under OCM reaction conditions towards methane activation, and how this is influenced by the dopant concentration in Li^+-doped TiO_2 catalysts. It has been shown that this catalyst exhibits good activity, selectivity, and stability characteristics for methane partial pressures in the range of 0.3–0.5 bar. Hydrocarbon yields in the range of 10–15% have been obtained over this catalyst at temperatures as high as 900°C and methane pressures of up to 0.5 bar. Kinetic studies under OCM reaction conditions, as well as transient studies on the reactivity of CH_4 and C_2H_6 with the lattice oxygen of the Li^+-doped TiO_2 catalyst, have been reported previously (*2, 7*).

The steady-state tracing technique, which involves an abrupt switch from a reactant species in the feed to a corresponding isotopically labeled species, has recently found application in the investigation of the mechanism of oxidative coupling of methane (*5, 8–10*). These studies revealed that the amount of adsorbed methane under reaction conditions is practically zero, whereas there is a large reservoir of surface/subsurface oxygen species which participate in the formation of the undesired CO and CO_2 products. Other transient isotopic experiments conducted under conditions relevant to methane coupling have also been performed to evaluate oxygen isotope transfer rates and to study the interaction of CH_4 with the catalyst surface (*1, 11–13*). In the present work, transient experiments with the use of $^{18}O_2$ have been conducted to study the mobility characteristics (diffusivity, activation energy of diffusion, transfer rate) of bulk lattice oxygen, and to relate this to methane activity under OCM conditions, as a function of Li^+-dopant concentration.

Lithium-doped TiO_2 catalysts were prepared and characterized in terms of surface area (BET), electrical conductivity and activation energy of electron conduction, surface acidity and basicity, and bulk composition (XRD) and surface composition (XPS), as described in detail elsewhere (*2*). Transient isotopic experiments with $^{18}O_2$ were performed in a flow system which has been

0021-9517/93 $5.00

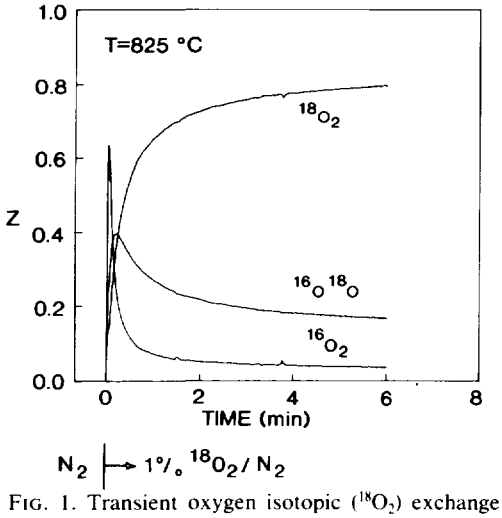

FIG. 1. Transient oxygen isotopic ($^{18}O_2$) exchange experiment according to the delivery sequence $N_2 \rightarrow$ 1 mol% $^{18}O_2/N_2(t)$. T = 825°C, 1 wt% Li_2O-doped TiO_2 catalyst.

described elsewhere (*7*). Continuous monitoring of the transient responses obtained from the reactor was performed by on-line mass spectrometer (VG Quadrupoles, Sensorlab 200D) equipped with a fast response inlet capillary system. The reactor system used for transient studies has been described earlier (*7*). For the $^{18}O_2$ transient exchange experiments, the following conditions were used: 30 cm^3/min (ambient conditions) total flow rate of N_2 switched to 30 cm^3/min of 1 mol% $^{18}O_2/N_2$ mixture, catalyst weight 1.0 g, total pressure 1 bar, temperature range 650–850°C. The transient responses of $^{16}O_2$, $^{16}O^{18}O$, and $^{18}O_2$ gases are reported as dimensionless concentration, Z, vs time. For instance,

$$Z_{^{16}O^{18}O}(t) = \frac{y_{^{16}O^{18}O}}{y_{^{16}O_2} + y_{^{16}O^{18}O} + y_{^{18}O_2}}, \quad (1)$$

where y is the mole fraction of a given gaseous oxygen species. Thus, at a given time t, the $Z(t)$'s of all three oxygen gaseous species add up to 1.0. Initial rates of methane conversion have been obtained in a conventional flow apparatus described earlier (*2*).

Figure 1 shows oxygen transients obtained at 825°C after the gas flowing over the 1 wt% Li_2O/TiO_2 catalyst was changed from N_2 to 1% $^{18}O_2/N_2$ mixture. At the switch to the isotopic mixture there is a rapid exchange of ^{16}O with ^{18}O atoms, which leads to the production of $^{16}O^{18}O$ gas. The ^{18}O atoms are likely formed by dissociation of molecular $^{18}O_2$ on the surface. In addition, there is a failure of the $^{16}O^{18}O$ signal to relax back to zero even for times greater than 20 min, not shown in Fig. 1, and the rate of production of $^{16}O^{18}O$ gas after about 5 min of exchange declines slowly. These results suggest that there exists an ^{16}O source which feeds the surface with ^{16}O atoms. This source is the bulk of the doped-TiO_2 catalyst. It should be noted that no leaks from the reactor or the gas lines were present which could partly account for the ^{16}O source. In contrast to the $^{16}O^{18}O$ transient response, the $^{16}O_2$ response shows a different behaviour; in this case there is a rapid decline of the $^{16}O_2$ signal under exchange conditions towards its background value.

Similar results with respect to the shape of the oxygen transients of Fig. 1 have been observed at other temperatures in the range of 700–840°C, as well as over the 2 and 4 wt% Li_2O/TiO_2 and undoped TiO_2 catalysts. However, the most important effect of temperature and catalyst composition was to change the value of the pseudosteady state rate of production of $^{16}O^{18}O$ gas as shown in Table 1.

Following the analysis given by Peil *et al.* (*5*) of an experiment similar to that described in Fig. 1, the average diffusivity of lattice oxygen in the solid can be estimated based on the offset (pseudosteady state) value of the $^{16}O^{18}O$ transient response. This is given by the relationship (*5*).

$$D = \pi t_{s.s.} \left(\frac{N_A}{C_{A_0}}\right)^2, \quad (2)$$

where $t_{s.s.}$ (sec) is the time required for the $^{16}O^{18}O$ signal to reach its pseudosteady state value, N_A (moles/cm^2 · sec) is the flux of atomic oxygen at the catalyst surface from

TABLE 1

Rate of Formation of $^{16}O^{18}O$ and Lattice Oxygen Availability as Well as Diffusivity as Determined from $^{18}O_2$-Exchange Experiments

Catalyst	T(°C)	Rate of formation[a] of $^{16}O^{18}O$ (moles/m^2 · s) × 10^8	Lattice oxygen availability (equivalent number of layers)[b]	Oxygen Diffusivity (cm^2/s) × 10^{18}	Activation energy of bulk lattice oxygen diffusion (kcal/mol)
TiO_2	730	2.9	1.1	0.6	
	760	6.6	2.4	3.4	110 ± 5
	780	10.6	3.7	8.7	
1 wt% Li_2O/TiO_2	730	1.2	0.6	0.1	
	760	2.5	1.1	0.5	130 ± 5
	790	8.2	3.6	5.2	
	825	17.8	7.1	24.6	
2 wt% Li_2O/TiO_2	800	2.4	1.0	0.5	
	810	2.8	1.2	0.7	104 ± 5
	825	3.5	1.6	1.0	
	840	5.2	2.2	2.2	
4 wt% Li_2O/TiO_2	760	1.8	0.8	0.3	
	785	3.0	1.3	0.9	87 ± 5
	810	5.1	2.2	2.6	
	825	6.5	2.8	4.1	

[a] Based on the pseudosteady state value of $^{16}O^{18}O$ transient as explained in the text.
[b] Based on the integration of $^{16}O^{18}O$ transient response over up to 20 min of exchange.

the bulk, and C_{A_0} (moles/cm^3) is the initial concentration of atomic oxygen in the bulk. N_A is calculated by multiplying the $y_{^{16}O^{18}O}$ of the offset by the total molar oxygen flow (moles/sec) and dividing by the catalyst weight (g) and surface area (cm^2/g).

The specific rate of formation of $^{16}O^{18}O$ at pseudosteady state conditions, the equivalent number of mobile atomic oxygen layers exchanged by ^{18}O, and the oxygen diffusivity (based on Eq. (2)) as a function of catalyst composition and temperature are shown in Table 1. The equivalent number of mobile atomic oxygen layers is calculated by integrating the $^{16}O^{18}O$ transient response (for a time up to 20 min) and using a 6.7 Å^2/oxygen atom. The latter number is based on the lattice parameters of rutile TiO_2 and the number of surface oxygen atoms/unit cell. Assuming an Arrhenius expression for the diffusivity as a function of temperature, the activation energy of bulk lattice oxygen diffusion can be calculated. Figure 2 shows these results for 0, 1, 2 and 4 wt% Li_2O-doped TiO_2 catalysts. The activation energy values obtained are also given in Table 1.

Figure 3 shows initial rates of methane consumption, at methane conversions less than 5%, as a function of the Li_2O content of the catalyst. To illustrate the close correlation of the dependence of initial rate of methane consumption and activation energy of bulk lattice oxygen diffusion on the Li_2O content of the catalyst, the results of activation energy vs Li_2O content are also plotted in Fig. 3. The methane activity results correspond to a 900°C reaction temperature, a partial pressure of CH_4, P_{0,CH_4} = 0.5 bar, and a CH_4/O_2 feed ratio of 3.

The present transient oxygen-exchange experiments reveal that the lithium dopant concentration has a strong influence on the

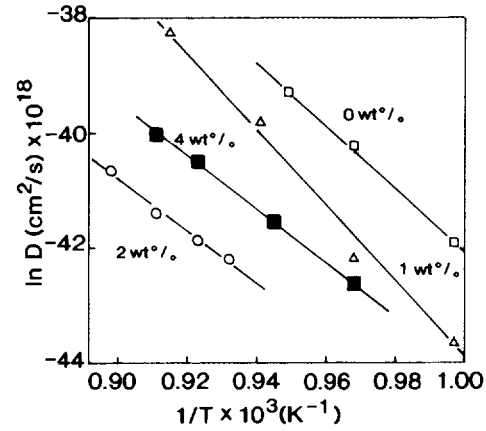

FIG. 2. Arrhenius plots of bulk lattice oxygen diffusivity as a function of Li^+-dopant concentration (wt% Li_2O).

bulk lattice oxygen mobility. This is demonstrated by the variation of the activation energy of bulk lattice oxygen diffusion (Fig. 2, Table 1). It was found that at the level of doping of ca. 1 wt% Li_2O an increase in the activation energy of lattice oxygen diffusion occurred, as compared to the value obtained for the undoped TiO_2, whereas at the level of doping of ca. 2 and primarily 4 wt% Li_2O a decrease in the activation energy occurred. To better understand the behaviour of lithium dopant concentration on the mobility of lattice oxygen of doped -TiO_2, some

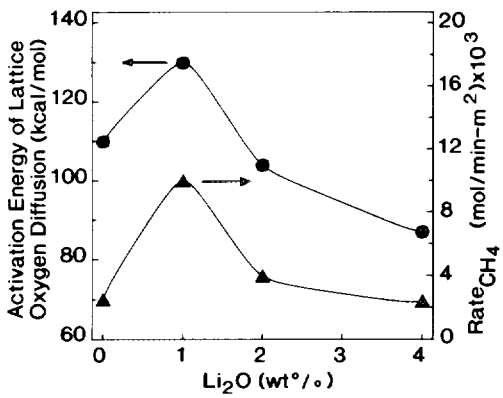

FIG. 3. Activation energy of lattice oxygen diffusion and initial specific rate of CH_4 conversion vs Li^+-dopant concentration (wt% Li_2O).

basic crystallographic information concerning rutile TiO_2 is mentioned. The rutile form of TiO_2 is a tetragonal crystal structure, in which each Ti^{4+} cation is surrounded by a slightly deformed oxygen octahedron, whereas each oxygen anion species, O^{2-}, is surrounded by three Ti^{4+} cations placed in the vertices of an isosceles triangle. The mobility of oxygen anion species around their lattice equilibrium positions is therefore primarily dependent on the electrostatic field created by the three Ti^{4+} cations (short range electrostatic interactions). When titania is doped with lithium cations, the latter are expected to (a) substitute for Ti^{4+} cations in their lattice positions, (b) occupy interstitial and/or defect site positions in the lattice, or (c) both of the above.

It is difficult to theoretically predict what might be the effect of dopant concentration on its distribution into the aforementioned lattice positions. It is therefore suggested that the observed increased activation energy value of bulk lattice oxygen diffusion of the 1 wt% Li_2O-doped TiO_2 catalyst must be due to an increase in the electrostatic force between oxygen anion species and their surrounding cations. This force arises from the presence of Li^+ cations at interstitial and/or defect sites in the vicinity of lattice oxygen anion species. It might be appropriate to say that at this level of doping, energy requirements impose occupancy of such positions by the majority of Li^+ cations. On further increase in the level of doping, substitution of Ti^{4+} by Li^+ cations seems to occur, causing, therefore, a decrease in the activation energy of bulk lattice oxygen diffusion, as observed over the 2 and 4 wt% Li_2O/TiO_2 catalysts, compared to the undoped TiO_2. X-ray diffraction measurements performed on the 1 and 4 wt% Li_2O-doped TiO_2 catalysts revealed that Li_2TiO_3 is present in the latter catalyst formulation, whereas no such indication was found for the former catalyst (*2*). The lower activation energy of lattice oxygen mobility observed in the 4 wt% Li_2O-doped TiO_2 compared to that of the undoped TiO_2 cata-

lyst may also be related to the presence of the Li_2TiO_3 phase.

In similar experiments to those presented in Fig. 1, Peil *et al.* (*5*) observed a large decrease in the activation energy of bulk lattice oxygen diffusion of MgO when the latter was doped with Li^+ cations (14 wt% Li/MgO). These results are similar to the present ones for undoped TiO_2 and 4 wt% Li_2O/TiO_2 catalysts. In (*5*) the authors suggested that the aforementioned behaviour was due in part to the creation of lattice defects upon Li^+ doping. In addition, the $^{16}O^{18}O$ transient responses obtained over Li/MgO (*5*) and Sr/La_2O_3 (*13*) were qualitatively similar to that shown in Fig. 1, and aspects of this transient response have been previously discussed in some detail (*5*). The diffusivity values reported in Table 1 should be treated with some caution since they depend on the choice of $t_{s.s.}$. However, it is clear from Eq. (*2*) that the activation energies of diffusion shown in Table 1 do not depend on uncertainties in the appropriate $t_{s.s.}$ value. The number of equivalent layers of lattice oxygen (surface/subsurface) which are mobile and exchange with gaseous oxygen in the range of 730 to 840°C is greater than 1, and in some cases it is of the order of several monolayers (Table 1). This result has also been obtained over MgO and Li/MgO systems (*5*) as well as La_2O_3 and Sr/La_2O_3 systems (*13*). It is important to note here that estimation of activation energies of lattice oxygen diffusion over the present series of Li^+-doped TiO_2 catalysts under OCM reaction conditions was impossible due to the absence of $^{16}O^{18}O$ signal upon the switch from CH_4/O_2 to $CH_4/^{18}O_2$ mixture (*9*).

Figure 3 reveals that a good correlation exists between catalytic activity (initial methane consumption rate) and lattice oxygen mobility, the latter characterized by the activation energy of lattice oxygen diffusion. The catalyst with the highest activation energy appears to be the most active. Steady-state tracing experiments over the present 1 wt% Li_2O/TiO_2 catalyst revealed that several layers of subsurface lattice oxygen participate in the formation of CO_2 under OCM reaction conditions (*9*). Even though it is difficult to know the extent of participation of precursor species derived from CH_4 in the CO_2 reaction pathway, as a result of the oxidation of C_2-hydrocarbon products to CO_2 (*7*, *9*), it may be suggested from the present results that activation of methane by $H^\cdot$ abstraction by oxygen species to form initially methyl radicals, and/or oxidation of the latter species to form CO_2, require less mobile surface/subsurface oxygen species, in accordance with what has been proposed earlier (*14*). It can be further speculated that the catalyst surface may possess $[Li^+O^-]$ centers which facilitate the stability of O^- species and which may be responsible for methane activation and/or nonselective oxidation processes. Such centers were first observed by Ito *et al.* (*15*) over the Li/MgO catalyst. It may also be appropriate to state that by increasing the Li_2O dopant concentration, Li_2TiO_3 is formed (*2*) at the expense of $[Li^+O^-]$ centers on the surface of the present 4 wt% Li_2O/TiO_2 catalyst. The possibility that O^- and O^{2-} species participate in the formation of CO_x products over other OCM catalytic systems has been reviewed recently (*1*).

REFERENCES

1. Sokolovskii, V. D., and Mamedov, E. A., *Catal. Today* **14,** 419 (1992), and references therein.
2. Efstathiou, A. M., Boudouvas, D., Vamvouka, N., and Verykios, X. E., *J. Catal.* **140,** 1 (1993), and references therein.
3. Akubuiro, E. C., and Verykios, X. E., *J. Phys. Chem. Solids* **50,** 17 (1989).
4. Dubois, J.-L., and Cameron, C. J., *Appl. Catal.* **67,** 49 (1990).
5. Peil, K. P., Goodwin, J. G., and Marcelin, G., *J. Catal.* **131,** 143 (1991).
6. Carreiro, J., and Baerns, M., *React. Kinet. Catal. Lett.* **35,** 309 (1987).
7. Efstathiou, A. M., Papageorgiou, D., and Verykios, X. E., *J. Catal.* **141,** 612 (1993).
8. Lacombe, S., Sanchez, J. G., Delichere, P., Mozzanega, H., Tatibouet, J. M., and Mirodatos, C., *Catal. Today* **13,** 273 (1992).
9. Lacombe, S., Efstathiou, A. M., Verykios, X. E., and Mirodatos, C., in preparation.
10. Ekstrom, A., and Lapszewicz, J. A., *J. Am. Chem. Soc.* **110,** 5226 (1988).

11. Cant, N. W., Lukey, C. A., and Nelson, P. F., *J. Catal.* **124,** 336 (1990).
12. Ekstrom, A., and Lapszewicz, J. A., *J. Phys. Chem.* **93,** 216 (1989).
13. Kalenik, Z., and Wolf, E. E., *Catal. Today* **13,** 255 (1992).
14. Solokovskii, V. D., *React. Kinet. Catal. Lett.* **35,** 337 (1987).
15. Ito, T., Wang, J.-X., Lin, C.-H., and Lunsford, J. H., *J. Am. Chem. Soc.* **107,** 5062 (1985).

A. M. EFSTATHIOU
D. PAPAGEORGIOU
X. E. VERYKIOS

Institute of Chemical Engineering and High Temperature Chemical Processes
Department of Chemical Engineering
University of Patras
26500 Patras, Greece

Received February 17, 1993; revised June 18, 1993